

## Mean-field theory of oxygen-vacancy ordering in $\text{YBa}_2\text{Cu}_3\text{O}_{7-\delta}$

L. T. Wille

*Materials and Chemical Sciences Division, Lawrence Berkeley Laboratory, Berkeley, California 94720  
and Department of Physics, Florida Atlantic University, Boca Raton, Florida 33431\**

(Received 30 November 1988)

A high-temperature phase diagram and various correlation functions have been calculated for the partially occupied oxygen sublattice in the CuO basal plane of  $\text{YBa}_2\text{Cu}_3\text{O}_{7-\delta}$  ( $0 \leq \delta \leq 1$ ). This structure is modeled as a two-dimensional Ising system with repulsive first-neighbor and anisotropic, competing second-neighbor interactions. These interactions are selected to guarantee the stability (at zero temperature) of the two experimentally observed orthorhombic phases: a single-cell structure (with Cu-O chains parallel to the  $b$  axis) at  $\delta=0$  and a double-cell structure (with regularly spaced missing chains) at  $\delta=0.5$ . The calculations are performed in the four- and five-point approximation of the cluster-variation method. The results are in good agreement with available experimental information.

### I. INTRODUCTION

Although more than two years have elapsed since the initial discovery<sup>1</sup> that triggered a worldwide flurry of activity, the mechanism for superconductivity and the essential ingredients in the so-called high- $T_c$  materials remain somewhat of a mystery. The 1-2-3 compound  $\text{YBa}_2\text{Cu}_3\text{O}_{7-\delta}$  ( $T_c \approx 90$  K) (Refs. 2 and 3) and those related to it by various Y and Cu substitutions contain both  $\text{CuO}_2$  planes (actually, dimpled sheets) and planes with parallel CuO chains. At first it was believed that both features were essential for high-temperature superconductivity, but the subsequent discovery of the Tl-Ca-Ba-Cu-O ( $T_c \approx 125$  K) (Ref. 4) and Bi-Ca-Sr-Cu-O systems ( $T_c \approx 115$  K) (Ref. 5) disproved this assumption, since neither of these systems contains chain layers. It is now generally accepted that in all of these materials the  $\text{CuO}_2$  planes are the crucial ones as far as the high superconducting transition temperature and current-carrying capacity are concerned, but that these two quantities are extremely sensitive to the remainder of the structure, in particular to the amount of ordering in the chain layers in the 1-2-3 structure. Moreover, to illustrate the complexities that still remain, it is also believed that the presence of Cu is not a prerequisite for high- $T_c$  superconductivity, following the discovery of the superconducting perovskite  $\text{Ba}_{0.6}\text{K}_{0.4}\text{BiO}_3$  ( $T_c \approx 30$  K).<sup>6</sup>

The present paper is concerned with the order-disorder transformation in the CuO basal plane of  $\text{YBa}_2\text{Cu}_3\text{O}_{7-\delta}$ . As just mentioned, it is not this plane that is responsible for superconductivity, but it has now been amply shown<sup>7-12</sup> that the state of order in the basal plane has a dramatic effect on the superconducting properties. Only 50% of the oxygen sites in the plane are occupied when  $\delta=0$  and, depending on the thermal treatment of the material, these oxygen sites can be occupied at random or in an ordered fashion. In the completely disordered state the compound has overall tetragonal symmetry and is not superconducting, while in the fully ordered state (for  $\delta=0$ ) infinite Cu-O chains parallel to the  $b$  axis develop

[see Fig. 1(a)] and the resulting orthorhombic material is a 90 K superconductor. Moreover, as  $\delta$  is increased,  $T_c$  at first remains constant, then abruptly drops to 60 K when  $\delta \approx 0.3$ , exhibits a second plateau and vanishes quickly for  $\delta \leq 0.7$ .<sup>10,11</sup> The second plateau coincides with a dip in the room-temperature resistivity of the material, which is indicative of a short-range-ordering mechanism in that concentration range. These findings clearly show the important, indirect role that the chain layer plays for the superconducting properties of  $\text{YBa}_2\text{Cu}_3\text{O}_{7-\delta}$ . Knowledge of the phase diagram for the CuO basal plane and ensuing thermodynamic properties may help to test various proposed theories of high- $T_c$  superconductivity and will of course also be of great help in sample preparation and improvement.

The thermodynamics of oxygen ordering and the resulting chain formation in  $\text{YBa}_2\text{Cu}_3\text{O}_{7-\delta}$  have been the subject of several recent theoretical studies.<sup>13-25</sup> In all of this work it is assumed that, as far as the ordering behavior is concerned, the problem can be reduced to a purely two-dimensional one. One is thus led to an Ising type of problem involving occupied and vacant oxygen sites and the various treatments differ mainly in the choice of the interaction parameters and the statistical mechanical approach used. The possible choices and details of the present procedure (based on the cluster variation method)<sup>26</sup> will be outlined in Secs. II and III, respectively. The resulting phase diagram and oxygen correlation functions are presented in Sec. IV. Finally, the paper closes with a discussion and summary (Sec. V). Some of the results presented here have already been briefly described in a previous Letter.<sup>17</sup> Attention is also drawn to a recent paper<sup>27</sup> in which some other choices of parameters are investigated.

### II. MODEL

In order to obtain a tractable model to describe oxygen ordering in  $\text{YBa}_2\text{Cu}_3\text{O}_{7-\delta}$  a number of simplifying assumptions need to be made such that they capture the

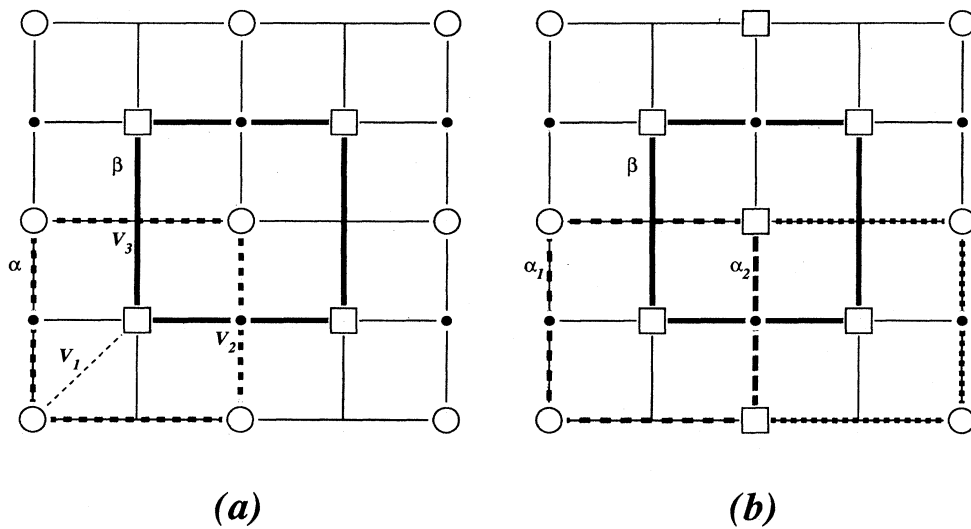


FIG. 1. Two-dimensional model of the  $\text{YBa}_2\text{Cu}_3\text{O}_{7-\delta}$  basal plane underlying the present work. Black dots denote Cu ions; open circles: oxygens; and open squares: vacancies (unoccupied oxygen sites). (a) Ordered structure at  $\delta=0$  contains Cu-O chains parallel to the  $b$  axis and consists of two oxygen sublattices  $\alpha$  and  $\beta$ . (b) Double-cell phase at  $\delta=0.5$  is obtained from that at  $\delta=0$  by removing alternating chains, and gives rise to three oxygen sublattices  $\alpha_1$ ,  $\alpha_2$ , and  $\beta$ . Effective pair interactions  $V_1$ ,  $V_2$ , and  $V_3$  coupling the oxygen sites are indicated. The small orthorhombic distortion ( $a \neq b$ ) is neglected in the calculations.

essential physics of the problem. In previous work<sup>13–25</sup> it has been shown that many of the experimental observations can be reproduced by using a purely two-dimensional Ising model for a single CuO basal plane, assuming that the parallel planes perpendicular to the  $c$ -axis are uncoupled. The latter is most certainly not true, for if it were, the basal planes would be equally probable to form chains parallel to the  $a$  and  $b$  axis and the resulting macroscopic structure would be tetragonal. However, the coupling of the basal planes is expected to be elastic in origin and elastic interactions have been neglected in the various statistical treatments. Likewise, the small rectangular distortion upon going from a tetragonal ( $a=b$ ) to an orthorhombic ( $a \neq b$ ) unit cell is ignored and consequently twin boundaries will not be described well in the present model. The main effect of elasticity on the phase diagram would be to renormalize transition temperatures and hence one may reasonably expect to obtain the correct topology when elastic interactions are ignored.

The model chosen in this and previous work is represented in Fig. 1(a). Shown is the completely ordered structure for  $\delta=0$ , consisting of three sublattices: a Cu sublattice (black dots, assumed to be rigid), a fully occupied oxygen sublattice ( $\alpha$ , with open circles representing oxygens), and an empty sublattice ( $\beta$ , containing vacancies denoted by open squares). The oxygen concentration of the basal plane will be denoted by  $c_{\text{O}}$  and is equal to  $\frac{1}{2}(1-\delta)$ , provided that oxygens are only removed from the basal plane, which is strictly speaking only true for sufficiently small  $\delta$ . Next it is necessary to define ordering interactions that couple the oxygen sites. In the

present and previous<sup>13–18</sup> work nearest- ( $V_1$ ) and next-nearest- ( $V_2, V_3$ ) neighbor interactions were considered. The only role of the Cu ions is to differentiate between  $V_2$  and  $V_3$ , and the Cu sublattice henceforth disappears from the formalism. A number of other authors<sup>19,20,22–25</sup> have assumed that only  $V_1$  is important, neglecting  $V_2$  and  $V_3$  altogether, while others<sup>21</sup> did consider second-neighbor coupling, but with  $V_2=V_3$ . As can be seen, both approaches ignore the role of the Cu atoms on the O bonding and it has been found<sup>14</sup> that these models are not able to reproduce all the experimentally observed structures. Indeed, various groups using a diversity of experimental techniques<sup>28–37</sup> have observed a cell-doubled phase near  $\delta=0.5$ , the basal plane of which (for  $c_{\text{O}}=0.25$ ) is shown in Fig. 1(b). It is to be noted that the resulting structure still contains Cu-O chains parallel to the  $b$  axis and is obtained from that at  $\delta=0$  by eliminating every other Cu-O chain. Thus the  $\alpha$  sublattice is now split up further in two sublattices:  $\alpha_1$ , completely occupied, and  $\alpha_2$ , which has all its oxygens removed. Both structures have orthogonal  $p2mm$  symmetry and will be denoted by OrthoI (at  $\delta=0$ ) and OrthoII (at  $\delta=0.5$ ) in the remainder of this paper.

The interaction parameters  $V_r$  ( $r=1,2,3$ ) are customarily called effective pair interactions (EPI's) in theories of alloy phase formation and stability<sup>38</sup> and can be given an operational definition as follows:

$$V_r = \frac{1}{4} [W_r(\circ - \circ) + W_r(\square - \square) - 2W_r(\circ - \square)], \quad (1)$$

where the  $W_r$  denote total energies of a system containing the specified pair in the respective positions, with all

other oxygen sites randomly occupied by oxygens and vacancies, at fixed overall oxygen concentration  $c_O$ . It is straightforward to define, in a similar fashion, more general effective cluster interactions (ECI's) involving more than two sites, but this has not been proven necessary for the system under study. Note that all of these interactions are strictly speaking concentration dependent<sup>39-41</sup>—a complication that has been ignored in all studies of the present problem to date. It is known that for metallic alloys the EPI's form a rapidly convergent series as a function of atomic separation, in spite of the fact that the cohesive energy of a transition metal cannot be expressed in terms of pair potentials.<sup>42</sup> Upon taking the difference of the cohesive energies  $W_r$  (quantities of the order  $10^3$  Ry), a large cancellation occurs and one is left with short-ranged EPI's (of the order mRy). However, it is not clear that the same will still be true in a strongly ionic system, such as  $YBa_2Cu_3O_{7-\delta}$ . Again, the restriction of the  $V$ 's to just three values can be justified *a posteriori* by the good experimental agreement. On the other hand, one consequence of the ionic nature of the system is that methods<sup>42-44</sup> which were successfully used to calculate EPI's for transition metal alloys fail in the present case because of the difficulty to model charge transfer.

It can be easily seen from the definition (1) that a positive (negative) EPI gives rise to a repulsive (attractive) interaction. Thus, from the observed ground-state in Fig. 1(a) one can conclude that  $V_1$  must be positive in order to produce  $\circ-\square$  nearest-neighbor pairs. From Fig. 1(b) it can be seen that one must have an attractive interaction along the Cu-O chains ( $V_2 < 0$ ) and a repulsive interaction between fully occupied chains ( $V_3 > 0$ ). Moreover, it is plausible to take both  $V_2$  and  $V_3$  less than  $V_1$  in magnitude, since otherwise the restriction of the interactions to nearest and next-nearest neighbors only is not warranted. These conclusions have been put on a more rigorous footing by performing a full ground-state analysis,<sup>14</sup> using  $V_1$  as a scaling parameter. If other ground states are found to exist it will be necessary to extend the interaction parameter set. In particular, structures have been observed at finite temperature containing more complicated chain arrangements,<sup>33,36</sup> as well as a  $2\sqrt{2} \times 2\sqrt{2}$  cell<sup>45-46</sup> at  $\delta=0.125$ . If these are indeed stable configurations, a modified set of EPI's including further neighbor coupling and/or cluster interactions may be necessary. However, in view of the extremely slow kinetics at low temperatures, the present author prefers the explanation that those structures correspond to frozen-in metastable configurations. (Note that Khachatryan *et al.*<sup>22-24</sup> argue that the double-cell phase which is here taken to be a stable ground-state, is in reality metastable and that therefore it is not necessary to consider different  $V_2$  and  $V_3$ . Such questions are very difficult, if not impossible, to settle experimentally. To the author it appears that the observed domains are sufficiently large, so that it is likely that they correspond to true equilibrium.)

Ultimately, the effective pair interactions are electronic in origin and can, in principle, be determined from electronic structure calculations.<sup>38-41</sup> Such calculations would be able to settle the question whether  $V_3$  is nega-

tive (double-cell phase metastable) or positive (double-cell phase true ground-state) and, if sufficient accuracy can be accomplished, could determine the magnitude of the further-neighbor and/or cluster interactions. No calculated values are available as yet, but some arguments can be given to justify the choice  $V_1 > 0$ ,  $V_2 < 0$ ,  $0 < V_3 < V_1$ . The Cu atoms in the chain layer have oxygen atoms above and below them along the  $c$  axis. (These oxygens are fairly inert for small  $\delta$ , but are progressively removed as  $\delta$  increases—a problem that will be addressed below.) Bonded to two oxygens in the chains, the  $Cu^{2+}$  ions thus have perfect square coordination in the OrthoI phase and this is energetically the most stable configuration. (This also explains why substitution of  $Cu^{2+}$  by a trivalent ion such as  $Fe^{3+}$  will lead to breakup of the chains and the measured detrimental effect of even relatively small Fe concentrations on  $T_c$ .) Removing or adding an oxygen atom to this arrangement, or distorting the square will be costly in energy. Hence, based on the coordination chemistry alone, one expects a positive  $V_1$  and a negative  $V_2$ , with  $V_3$  undetermined but presumably small. However, the previous reasoning ignores the Coulomb repulsion between oxygen atoms. If this were taken into account separately, it would lead to a positive  $V_1$  and  $V_3$ , with  $V_2$  undetermined, but small. The combined effect of these interactions will thus lead to a large positive  $V_1$ , and smaller  $V_2 < 0$  and  $V_3 > 0$ , precisely as the ground-state analysis<sup>14</sup> predicted on the basis of stable OrthoI and OrthoII phases. Since no calculated values for the EPI's are known, the "canonical" choice  $V_2 = -\frac{1}{2}V_1$ ,  $V_3 = \frac{1}{2}V_1$  has been made in the remainder of this paper. One can reasonably expect that this will at least give the correct topology of the phase diagram, and, in fact, the good fit to various experimentally observed quantities seems to indicate that these values are fairly accurate.

### III. STATISTICAL METHOD

Except in very special instances the two-dimensional Ising model with second-neighbor interactions present cannot be solved exactly,<sup>47</sup> and hence approximate methods have to be used. In the present and previous<sup>15-18</sup> work the cluster variation method (CVM) (Ref. 26) has been employed to this end. The CVM is essentially a mean-field theory in which the local order in a small cluster is treated exactly, but larger clusters are treated in the superposition approximation. By taking larger and larger clusters one generates a hierarchy of approximations, which in the infinite cluster limit would give exact results. In practice, for computational reasons, one has to truncate the free energy expansion at a fairly small cluster size. Various levels of the CVM has been employed by previous authors to the present oxygen-vacancy ordering problem: the Bragg-Williams approximation<sup>23-24</sup> (CVM-point approximation), the quasichemical approach<sup>19,20</sup> (CVM-pair approximation) and the square approximation.<sup>21,25</sup> With both  $V_2$  and  $V_3$  present and opposite in sign it turns out to be essential to include both square and centered square clusters in the formalism: this is the four- and five-point approximation that has been used in our earlier papers.<sup>15-18</sup> All inequivalent

positions of these basic clusters within the given structure have to be determined, as well as all subclusters. These are shown in Fig. 2, with the four-point clusters in dashed lines and the five-point clusters in solid lines. Both types can occur in two inequivalent positions: the first ones either centered on a Cu atom or not, the second ones associated with the  $\alpha$  or  $\beta$  sublattice. Various oxygen sites have been labeled in accordance with the CVM framework, to be explained below.

After its introduction by Kikuchi<sup>26</sup> the CVM formalism was considerably simplified by Barker<sup>48</sup> and by Hijmans and de Boer.<sup>49</sup> The present work closely follows the latter two references, but uses the correlation function expansion of Sanchez and co-workers.<sup>50-51</sup> (For a tutorial discussion of the CVM as applied to the present problem, see Ref. 52.) Quite generally, the equilibrium configuration of a condensed system (at fixed concentration) can be obtained by minimizing the free-energy functional

$$F = \langle E \rangle - kT \ln \Omega, \quad (2)$$

where  $\Omega$  is the number of possible configurations with the same internal energy  $\langle E \rangle$ . The different levels in the CVM hierarchy, correspond to including larger and larger clusters in an approximate expression for  $\Omega$ . Hence, in this approach the free energy per atom can be written as

$$F = \sum_{r=1,2,3} n_r V_r \xi^r - kT \sum_j \gamma_j \sum_J x_j(J) \ln x_j(J). \quad (3)$$

Here  $\xi^r$  are the pair-correlation functions for nearest ( $\xi_2$ ) and next-nearest ( $\xi_3$ ) neighbors, corresponding to the chosen EPI  $V_r$ , and  $n_r$  is the number of such pairs per site. The sum over  $j$  in the second term runs over all subclusters of the basic ones. The  $x_j(J)$ , with  $J$  running over all possible occupancies of cluster  $j$ , are cluster concentrations, which can be expressed in terms of cluster correlation functions  $\xi$ , the latter being the independent variables of the problem (see below). The  $\gamma_j$  are the Kikuchi-Barker coefficients, which can easily be calculated recursively, as follows:<sup>48</sup>

$$\gamma_L = -m_L, \quad (4a)$$

$$\gamma_l = -m_l - \sum_{i=l+1}^L m_l^i \gamma_i, \quad (4b)$$

where  $m_l$  is the number of clusters of type  $l$  per lattice site,  $m_l^i$  is the number of subclusters of type  $i$  contained in that of type  $l$  and  $L$  labels the basic cluster. These coefficients are purely geometric quantities: they can be calculated once and for all for the disordered state (in the present case one can even ignore the Cu atoms). In the ordered states (OrthoI and OrthoII, in the present case) the cluster types are further subdivided, but the  $\gamma$ 's remain unchanged (if care is taken to normalize with respect to the same unit cell). For the case in which the Cu atoms are ignored, the Kikuchi-Barker coefficients are given in Table I and the appropriate weight factor for use in the entropy formula is<sup>52</sup> (now normalized per unit cell)

$$\Omega_0 = \frac{\{\text{four-point}\}^8}{\{\text{five-point}\}^4 \{\text{five-point}\}^2 \{\text{five-point}\}^2} \quad (5)$$

where each of the brackets  $\{j\}$  stands for a product of factorials of the form  $\prod_j [N x_j(J)]!$ ,  $N$  being the total number of lattice points considered. Substitution of this expression in (2), and application of Stirling's formula yields Eq. (3). The cluster probabilities are not all independent, which would lead to a rather awkward constrained minimization problem. However, it is fairly straightforward to express them in terms of a set of independent cluster correlation functions.<sup>50</sup> The transformation between the two representations [for the clusters occurring in (5)] is given in Table II. The arguments  $i, j, k, \dots \in \{-1, +1\}$  label sites according to Fig. 2 and run over all possible configurations (+1 refers to an oxygen atom, -1 to a vacancy).

In the tetragonal (disordered) structure the entropy weight-factor becomes<sup>52</sup>

$$\Omega_T = \frac{\{\text{four-point}\}^4 \{\text{five-point}\}^4}{\{\text{five-point}\}^4 \{\text{five-point}\} \{\text{five-point}\} \{\text{five-point}\}^2}, \quad (6)$$

since some of the combinatorial factors split up when Cu's are introduced; in particular one now has to distinguish between clusters 5 and 5' (in the numerator) and 8 and 8' (second and third term in the denominator). In the OrthoI ordered phase one has to distinguish between the  $\alpha$  and  $\beta$  sublattice and 25 different cluster types are obtained. It is easy to show that the relevant statistical weight formula now is<sup>52</sup>

$$\Omega_{OI} = \frac{\{\text{four-point}\}^2 \{\text{five-point}\}^2 \{\text{five-point}\}^2 \{\text{five-point}\}^2}{\{\text{five-point}\}^4 \{\text{five-point}\} \{\text{five-point}\} \{\text{five-point}\} \{\text{five-point}\}}. \quad (7)$$

Thus the CVM free energy contains 25 (independent) correlations functions. Since the minimization is done at fixed concentration

$$c_O = \frac{1}{2}(\xi_1^\alpha + \xi_1^\beta), \quad (8a)$$

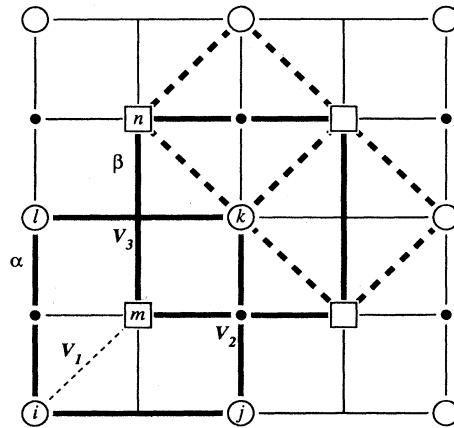


FIG. 2. Basal-plane model with sites labelled according to CVM formalism. The basic four-point (dashed line) and five-point (solid line) clusters are indicated in the two possible inequivalent positions.

TABLE I. Kikuchi-Barker coefficients  $\gamma_i$  for two-dimensional square Ising problems in the four-point and five-point approximation of the CVM (see text and Ref. 52).






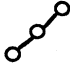



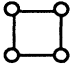
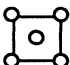
$j$	Cluster	$m_i$	$j:$	1	2	3	4	5	6	7	8	9	10	11	$\gamma_i$
1		1		1	2	2	2	3	3	3	4	4	4	5	0
2		2			1	0	0	2	2	0	4	3	0	4	-2
3		2				1	0	1	0	2	2	2	4	4	0
4		2					1	0	1	1	0	1	2	2	0
5		4						1	0	0	4	2	0	4	4
6		2							1	0	0	1	0	2	0
7		4	$m_j$							1	0	1	4	4	0
8		1									1	0	0	0	-1
9		4										1	0	4	0
10		1											1	1	0
11		1												1	-1

TABLE II. Transformation formulas between cluster probabilities  $x_j(J)$  and correlation functions  $\xi$ , for those terms that occur in the CVM entropy expression for the square Ising model (see text).

$$\begin{aligned}
 x_2(i, m) &= \frac{1}{4} [1 + (i + m)\xi_1 + (im)\xi_2] \\
 x_5(i, j, m) &= \frac{1}{8} [1 + (i + j + m)\xi_1 + (im + mj)\xi_2 + (ij)\xi_3 + (ijm)\xi_5] \\
 x_8(i, j, m, n) &= \frac{1}{16} [1 + (i + j + m + n)\xi_1 + (im + mj + jn + ni)\xi_2 + (ij + mn)\xi_3 \\
 &\quad + (ijm + ijn + mni + mnj)\xi_5 + (ijmn)\xi_8] \\
 x_{11}(i, j, k, l, m) &= \frac{1}{32} [1 + (i + j + k + l + m)\xi_1 + (im + jm + km + lm)\xi_2 \\
 &\quad + (ij + jk + kl + li)\xi_3 + (ik + jl)\xi_4 + (ijm + jkm + klm + lim)\xi_5 \\
 &\quad + (imk + jml)\xi_6 + (ijl + ijk + klj + kli)\xi_7 \\
 &\quad + (ijlm + ijk m + kljm + klim)\xi_9 + (ijkl)\xi_{10} + (ijklm)\xi_{11}]
 \end{aligned}$$

one is left with a 24-dimensional unconstrained optimization problem. It is also convenient to define a long-range order parameter as

$$\eta = \frac{1}{2}(\xi_1^\alpha - \xi_1^\beta), \quad (8b)$$

which goes to zero in the disordered state. Finally, in the OrthoII phase the  $\alpha$  sublattice is divided further in  $\alpha_1$  and  $\alpha_2$ , some of the relevant clusters in (7) factorize and the entropy expression (normalized for the double unit cell, i.e., four atoms per unit cell), becomes<sup>52</sup>

$\Omega_{OII} =$

$$\frac{\{\text{circles}\}^2 \{\text{circles}\}^2 \{\text{circles}\}^4 \{\text{circles}\}^2 \{\text{circles}\}^2 \{\text{circles}\}^2 \{\text{circles}\}^2}{\{\text{squares}\}^4 \{\text{squares}\}^4 \{\text{circles}\} \{\text{circles}\} \{\text{circles}\}^2 \{\text{squares}\}^2 \{\text{squares}\}^2 \{\text{squares}\}^2} \quad (9)$$

The corresponding free energy now contains 41 correlation functions. Again it is convenient to eliminate the point correlation functions to obtain the (fixed) concentration:

$$c_O = \frac{1}{4}(\xi_1^{\alpha 1} + \xi_1^{\alpha 2} + 2\xi_1^\beta), \quad (10a)$$

and two long-range order parameters, for example,

$$\eta_1 = \frac{1}{2}(\xi_1^{\alpha 1} - \xi_1^{\alpha 2}), \quad (10b)$$

$$\eta_2 = \frac{1}{3}(\xi_1^{\alpha 1} - 2\xi_1^\beta). \quad (10c)$$

The first one is equal to zero in the OrthoI phase, and both tend to zero in the disordered state.

In the canonical ensemble, the CVM free energy (3) has to be minimized at fixed concentration  $c_O$  in each of the phases considered. Phase boundaries are located by determining intersections of the minimum free energy (with common normalization) for the various phases. Since it is formulated in terms of correlation functions, the CVM readily gives information about these quantities in the relevant regions. Finally, the chemical potential can also be calculated directly by taking the (analytic) derivative of the free energy (3) with respect to concentration. Note that it would have been equally convenient to formulate the problem in the grand canonical ensemble and minimize the grand potential at fixed chemical potential.

#### IV. RESULTS

The formalism described in the previous section has been used to calculate phase diagrams for  $V_2 = V_3 = -\frac{1}{2}V_1$  (Refs. 15 and 16) and for  $V_2 = -\frac{1}{2}V_1$ ,  $V_3 = \frac{1}{2}V_1$ .<sup>17</sup> The former case was studied as a test on the accuracy of the chosen CVM approximation for this type of problems, because "exact" results (obtained from renormalization group and Monte Carlo calculations) were available for comparison. The resulting phase diagram (without double-cell phase) consisted of a high-temperature second-order transition line between the orthorhombic (single-cell) and tetragonal phase, ending in a tricritical point below which phase separation occurs.<sup>15,16</sup> It was found that the overall topology was in precise

agreement with more accurate calculations, the main discrepancy being that the second-order transition line is much steeper in the exact calculations, leading to a tricritical point at oxygen concentration  $c_O = 0.30$ , while the CVM calculations put it at  $c_O = 0.19$ . It was also found that the miscibility gap for this two-dimensional system is much flatter in the exact calculations. These features are not unexpected for a mean-field theory such as the CVM, which will tend to smoothen out phase boundaries.<sup>53</sup> The topology of the phase diagram is also very similar to that obtained by Khachatryan *et al.*<sup>23,24</sup> by means of the Bragg-Williams method.

The high-temperature part of the CVM phase diagram for the case  $V_2 = -\frac{1}{2}V_1$ ,  $V_3 = \frac{1}{2}V_1$  is shown in Fig. 3. Again, one finds a second-order transition line between the disordered (tetragonal) phase and OrthoI. The double-cell phase (stable at  $c_O = 0.25$ , at zero temperature) gives rise to a phase equilibrium region that peaks near  $c_O = 0.25$  and which joins onto the second order line at a bicritical point. The long dashed line is an ordering spinodal:<sup>53</sup> the metastable continuation of the second-order transition line into the OrthoII region. The spinodal gives the limits of stability of an  $\langle 00 \rangle$  ordering wave operating on the  $\alpha$  and  $\beta$  sublattices.<sup>13</sup> It is a typical mean-field feature, due to a loss of the convexity property of the free-energy functional by making a cluster approximation. However, such instability lines are often used to interpret the kinetics of decomposition.<sup>22</sup> The double-cell region is found to be bounded by a first-order transition

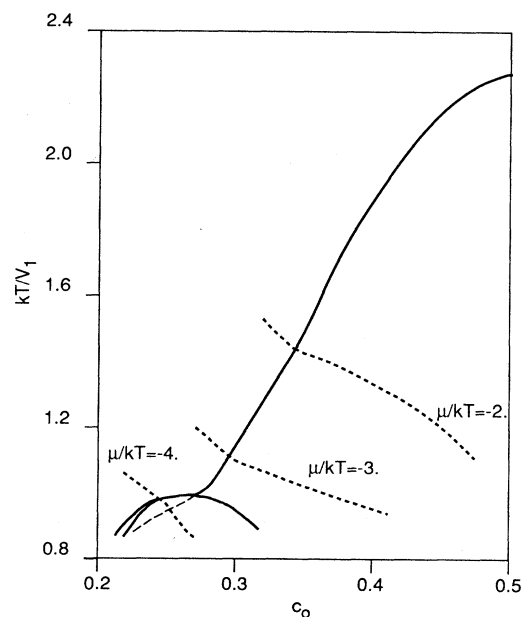


FIG. 3. CVM phase diagram for  $V_2 = -\frac{1}{2}V_2$ ,  $V_3 = \frac{1}{2}V_1$ . Phase boundaries between the tetragonal (disordered), OrthoI (single-cell) and OrthoII (double-cell) phases are indicated. Dashed lines designate different values of  $\mu/kT$  and corresponds approximately to lines of constant oxygen partial pressure. The fine dashed line is an ordering spinodal: a metastable extension of the second-order transition line into the double-cell region.

line between the OrthoII and the tetragonal phase, while the transition between OrthoI and OrthoII is calculated to be second order (as allowed by the Landau rules). No CVM data for temperatures below about  $kT/V_1=0.8$  could be calculated, because the algorithm becomes numerically unstable when too many correlation functions are close to the boundaries of the configurational simplex. However, in our previous Letter<sup>17</sup> conjectured extensions all the way to zero temperature were drawn. At these temperatures the kinetic of oxygen uptake and diffusion are so slow that the equilibrium state is probably not accessible. The second-order transition line joins smoothly onto the OrthoII phase boundaries. It is possible that a more accurate (i.e., non-mean-field) treatment will give a steeper line (by analogy to the case  $V_2 \equiv V_3 \equiv -\frac{1}{2}V_1$ ). This would be in agreement with the observation of Jorgensen *et al.*<sup>8</sup> that the OrthoI-tetragonal transition occurs at constant  $c_O \approx 0.30$ , independent of oxygen partial pressure. On the other hand, Specht *et al.*<sup>54</sup> measured transition temperatures and concentrations for  $p_{O_2} = 5 \times 10^{-3}$  to 1 atm. and found a noticeable increase in  $c_O$  at the transition with increasing  $p_{O_2}$ . In fact, when one of the data points of Specht *et al.* is used to fix the temperature scale, it is found that the resulting points fall very closely to the CVM curve.<sup>17</sup> However, since  $V_2$  and  $V_3$  were arbitrarily chosen (within the stability domain) such a good fit must be considered rather fortuitous. It is also to be kept in mind that the CVM will overestimate transition temperatures (since only fluctuations within the largest basic cluster are included): by approximately 5% at  $c_O = 0.50$  and usually more off stoichiometry.

Also shown in Fig. 3 are lines along which  $\mu/kT$  is constant, corresponding approximately to lines of constant oxygen partial pressure. Since  $YBa_2Cu_3O_{7-\delta}$  samples are often prepared by annealing under a constant oxygen atmosphere, these lines would be followed if equilibrium could be maintained at all temperatures. The relation between chemical potential and oxygen partial pressure ( $p_{O_2}$ ) is<sup>23</sup>

$$\mu = \mu^0 + \frac{1}{2}kT \ln p_{O_2}, \quad (11)$$

where  $\mu^0$  is the reference chemical potential (at  $p_{O_2} = 1$  atm.). The quantity  $\mu$  in (11) is actually a chemical potential difference,  $\mu_O - \mu_{\square}$ , and is precisely that calculated analytically in the CVM. Since  $\mu^0$  is not known (and is in general temperature dependent), lines of  $\mu/kT = \text{const}$  have been drawn in Fig. 3 to indicate approximate behavior for  $p_{O_2} = \text{const}$ . The curves cross from the disordered to the orthorhombic phase regions with a change in slope and tend to  $c_O = 0.50$  as  $T$  goes to zero. Very long annealing times (or large oxygen partial pressures) would be necessary, however, to reach this composition.

Correlation functions and cluster probabilities are obtained automatically by the CVM and it is interesting to investigate some of these variables. Point correlations, related to fractional site occupancies, are a measure of the long-range order in the system, while pair correlation functions measure short-range order (either within a given sublattice or between two sublattices). The frac-

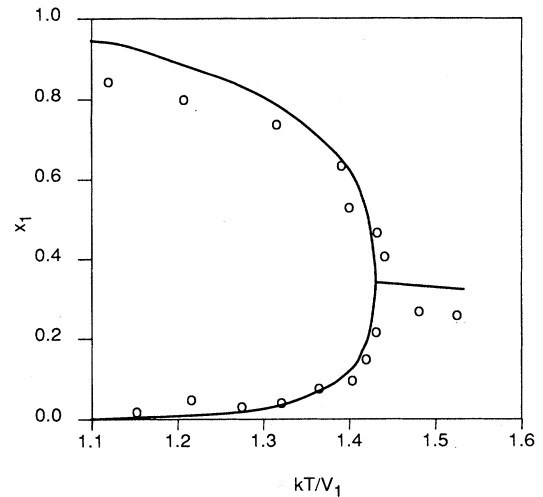


FIG. 4. Site occupancies for  $\mu/kT = -2$  as a function of temperature. In the disordered phase (above  $kT/V_1 \approx 1.43$ ) the oxygen sites are equivalent, while below that value an oxygen-rich (a) and oxygen-deficient (b) sublattice can be distinguished. The open circles are experimental data of Jorgensen *et al.*,<sup>8</sup> fitted to the calculated order-disorder temperature.

tional site occupancies on the  $\alpha$  and  $\beta$  sublattices at fixed  $\mu/kT = -2$ , are plotted as a function of temperature in Fig. 4. At low temperatures, two sublattices can be distinguished, the occupancy of one ( $\alpha$ ) tending to 1, that of the other ( $\beta$ ) going to 0. As the temperature is increased more and more disorder is evident (oxygen and vacancies situated on the "wrong" sublattice). Above  $kT/V_1 \approx 1.43$  the two sublattices are indistinguishable. At the transition point  $c_O \approx 0.34$  and from there on the oxygen concentration decreases monotonically with increasing  $T$ . Also indicated in Fig. 4 are experimental data of Jorgensen *et al.*,<sup>8</sup> scaled to give the correct disordering temperature. Again, the agreement is satisfactory, in particular since the experimental data at low temperature suffer from slow oxygen kinetics, hence the flattening out of the data for the oxygen-rich site at about 0.9.

Values of the oxygen-oxygen pair-probability function along the Cu-O chains at  $kT/V_1 = 0.9$  are shown in Fig. 5. This temperature was selected to be below the top of the double-cell region in order to include the effects of this phase on the short-range order. At this low temperature, ordering is almost complete at  $c_O = 0.5$ , the correlation function then decreases practically linearly with decreasing oxygen concentration. The second-order transition from OrthoI to OrthoII is encountered at  $c_O \approx 0.31$ . If the latter phase was not included in the calculations, the dashed line would be followed. This (metastable) curve is continuous until the spinodal is crossed, near  $c_O \approx 0.24$ , where the OrthoI sublattice "disorders," signaled by a change in slope in  $x_3^{\alpha}(\text{O-O})$ . If the double-cell phase is included (as it must, to describe equilibrium behavior), two  $\alpha$  sublattices must be distinguished. If the average value  $\frac{1}{2}(x_3^{\alpha 1} + x_3^{\alpha 2})$  is plotted, one finds a change in slope compared to  $x_3^{\alpha}$ , and a distinct shoulder is present. The curve now proceeds continuously until the OrthoII-tetragonal phase boundary is crossed (near

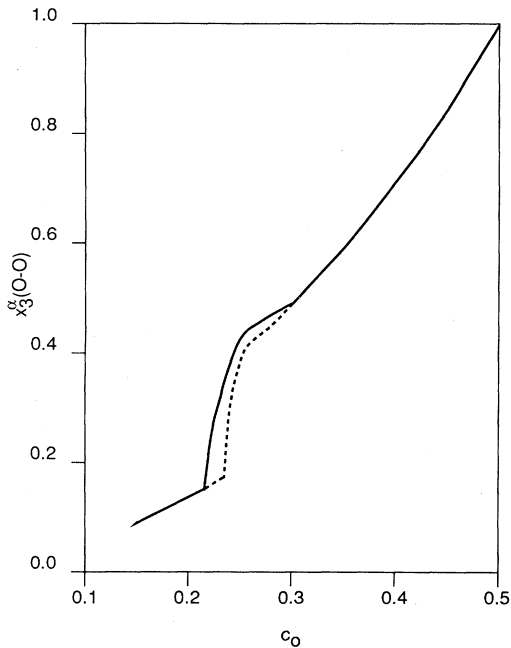


FIG. 5. Second-neighbor oxygen-oxygen pair probability along Cu-O chains at  $kT/V_1=0.9$ . Solid line: equilibrium probabilities; dashed line: metastable extension of single-cell phase.

$c_O \approx 0.21$ ). There, it joins (discontinuously) the curve for  $x_3^\alpha$  in the disordered state, also obtained in the absence of OrthoII. The small discontinuity across the first-order boundary, although evident in the numerical data, is too minute to be visible in the plot. Both the stable and metastable curve drop very quickly below  $c_O=0.26$ , which corresponds to the maximum of the OrthoII region. If  $x_3^{\alpha_1}$  is plotted separately, rather than the average over the two sublattices ( $\alpha_2$  being depleted in oxygen) a maximum is clearly visible in the same range.<sup>17</sup> One is led to conclude that the presence of the OrthoII phase gives rise to an increase in the short-range order along the Cu-O chains. Clearly, if OrthoII were not stable no such structure would be present. To illustrate this point further, Fig. 6 shows the same pair correlation function  $x_3^\alpha(O-O)$ , but now at a higher temperature  $kT/V_1=1.1$ , for which OrthoII is unstable at all concentrations. Sweeping down in concentration, the curve decreases monotonically and disorders with a discontinuity in slope near  $c_O \approx 0.30$ . The curve is in fact very similar to the metastable extension at  $kT/V_1=0.9$  (dashed line in Fig. 5), except that the disordering now occurs at a higher concentration, as it has to do at this higher temperature. Finally, to prove that the Cu-O chain ordering is the feature responsible for the short range ordering mechanism, Fig. 7 shows a second-neighbor pair probability for two oxygens on the a sublattice parallel to the a axis (no intervening Cu-atom) at  $kT/V_1=0.9$ . Again, a discontinuity is encountered when the OrthoI-OrthoII transition is met. Now the metastable extension (OrthoI) lies above the equilibrium curve, but both approach zero very quickly. This is of course as it has to be since one of the oxygen sites (that corresponding to  $\alpha_2$ ) is being depleted

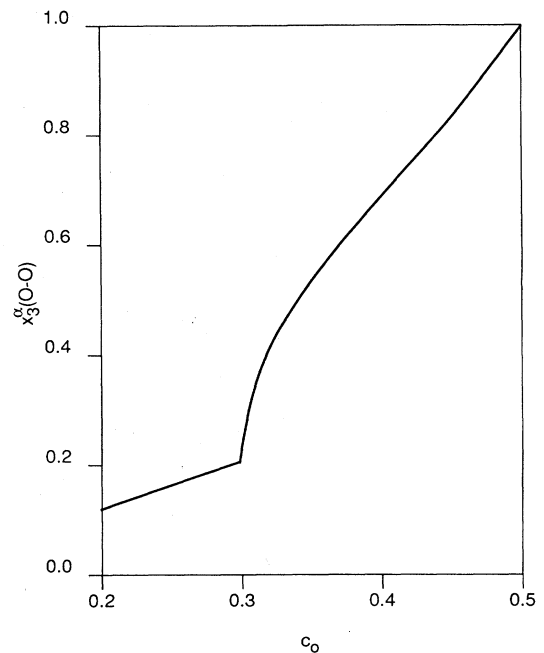


FIG. 6. Second-neighbor oxygen-oxygen pair probability along Cu-O chains at  $kT/V_1=1.1$  (no double-cell region present).

in the double-cell region. To sum up, because of the stability of OrthoII as an ordered ground state, one finds a plateau in the short-range order (here measured by  $x_3^\alpha$ ) around  $c_O \approx 0.30$ . This plateau is related to the Cu-O chain formation parallel to the  $b$  axis.

It seems very likely that the plateau in  $T_c$  near 60 K and the corresponding minimum in room-temperature resistivity, observed by Cava *et al.*<sup>10,11</sup> are related to the

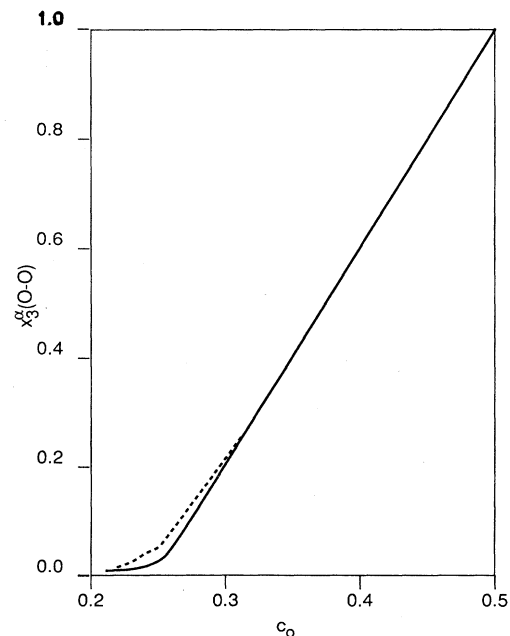


FIG. 7. Second-neighbor oxygen-oxygen pair probability parallel to a axis at  $kT/V_1=0.9$ .



short-range ordering mechanism just outlined. Again, kinetic considerations may limit the size of the ordered domains or even obliterate the effect altogether, depending on sample preparation. A purely electronic mechanism for the 60-K plateau has been proposed by Zaanen *et al.*<sup>55</sup> based on (zero-temperature) tight-binding calculations for the double-cell phase, further strengthening the evidence for a close connection between these two phenomena.

## V. CONCLUSIONS

It has been shown that a two-dimensional Ising model, with stable single- and double-cell configurations, is able to explain many experimental observations concerning the high-temperature superconductor  $\text{YBa}_2\text{Cu}_3\text{O}_{7-\delta}$ . Good qualitative and semiquantitative agreement is obtained for phase equilibrium lines and short- and long-range order parameters. However, it must be borne in mind that the model used is a very simple one, with only nearest- and next-nearest-neighbor interactions present, selected to guarantee the stability of the experimentally observed phases. This approximation is not necessarily based on the correct underlying Hamiltonian; for example, it may very well be that long-range interactions dominate the phase diagram.<sup>22-24</sup> Also, within the given model, the parameters used here were chosen rather arbitrarily and are by no means expected to be optimal.

A number of difficulties hamper comparison with experiment. It appears that many of the most interesting ordering phenomena happen at temperatures where kinetics are rather slow, so that equilibrium is not reached in the experiment, thus complicating the comparison with theoretical results from equilibrium thermodynamics. The sensitivity to sample preparation conditions also explains the sometimes conflicting findings from different groups. Moreover, there are problems relating the overall oxygen content ( $\delta$ ) to that in the basal plane ( $c_O$ ). First of all, extra oxygen will be present near the surface of the samples and in grain boundaries.<sup>56</sup> Moreover, it is also known that upon heating oxygen will be removed not only from the basal plane, but also from the sites just above and below the Cu atoms in that plane.<sup>57</sup> This will not only affect the ordering process in that plane, but it also means that  $c_O$  cannot directly be related to  $\delta$ . The relationship  $c_O = \frac{1}{2}(1 - \delta)$  will be obeyed quite closely for  $\delta \leq 0.5$ , but for larger values the deviations may be quite large.

Although the OrthoII phase has now been observed by many techniques, controversy still exists as to whether it is a true ground-state, or corresponds to a metastable phase, due to incomplete phase separation.<sup>24</sup> Again, slow kinetics make it very difficult to resolve this conflict. Perhaps the strongest piece of evidence for the stability of OrthoII is an indirect one: the observation of a plateau in  $T_c$  near 60 K (Refs. 10 and 11) almost exactly where

that phase is predicted to be stable. Both the models with ( $V_3 > 0$ ) and without ( $V_3 < 0$ ) OrthoII stable predict phase separation at low temperatures. For  $\delta \approx 1$ , the present model predicts separation between OrthoI and OrthoII, while the models with  $V_3 \leq 0$  predict tetragonal-OrthoI separation. TEM experiments by Chen *et al.*<sup>35</sup> show domains of OrthoII within an OrthoI matrix, but with very small domain size. Recently You *et al.*<sup>58</sup> performed x-ray diffraction measurements of  $\text{YBa}_2\text{Cu}_3\text{O}_{7-\delta}$  single crystals and found evidence for coexistence of phases with  $\delta \approx 0$  and  $\delta = 0.3$ , in agreement with the present model. If OrthoII is metastable, phase separation should be between phases with  $\delta \approx 0$  and  $\delta \approx 1$ . This is another indication for the stability of OrthoII at zero temperature.

Other ordered domains have been observed, and for those the same considerations apply. The model used here, only has ordered ground states for  $\delta = 0, 0.50$ , and 1.0. If other phases are found to be stable (at zero temperature), further neighbor and/or cluster interactions will have to be included. In particular, it is possible that a Coulomb- or screened-Coulomb repulsive interaction between oxygens is necessary. Under appropriate conditions such interactions may even give rise to a whole range of devil's-staircase phases. Further improvements, but no new ground states, may also result if elasticity and the full three-dimensional nature of the system is taken into account.

The central remaining question is how the chain layers influence the superconducting behavior located in the plane-layers. The calculations of Zaanen *et al.*<sup>55</sup> and experiments of Tokura *et al.*<sup>59</sup> indicate the importance of the hole count, although the issue is still by no means completely resolved. The present work has not addressed this problem at all, except by confirming the prediction of Cava *et al.*<sup>10,11</sup> for a correlation between short-range order and a plateau in  $T_c$ . As far as the oxygen ordering in the plane is concerned, it appears that the major features of this phenomenon are well described by the present model.

## ACKNOWLEDGMENTS

It is a pleasure to express my appreciation for stimulating discussions with R. J. Cava, J. D. Jorgensen, S. C. Moss, and G. Van Tendeloo. I also want to acknowledge the numerous contributions of my former colleagues at the University of California, Berkeley, including A. Berera, C. P. Burmester, D. de Fontaine, J. Kulik, and M. Sluiter. Work at Berkeley was supported by the Director, Office of Energy Research, Office of Basic Energy Sciences, Materials Sciences Division of the U.S. Department of Energy, under Contract No. DE-AC03-76SF00098. The work at Florida Atlantic University was supported by Grant No. MDA-972-88-J-1006 from the U.S. Defense Advanced Research Projects agency (DARPA).

\*Present address.

<sup>1</sup>J.G. Bednorz and K. A. Muller, *Z. Phys. B* **64**, 189 (1988).

<sup>2</sup>M. K. Wu, J. R. Ashburn, C. J. Torng, P. H. Hor, R. L. Meng, L. Gao, Z. J. Huang, Y. Q. Wang, and C. W. Chu, *Phys. Rev.*

*Lett.* **58**, 908 (1987).

<sup>3</sup>R. J. Cava, B. Batlogg, R. B. van Dover, D. W. Murphy, S. Sunshine, T. Siegrist, J. P. Remeika, E. A. Rietman, S. Zahurak, and A. P. Espinosa, *Phys. Rev. Lett.* **58**, 1676

- (1987).
- <sup>4</sup>Z. Z. Sheng, A. M. Hermann, A. El Ali, C. Almasan, J. Estrada, T. Datta, and R. J. Matson, *Phys. Rev. Lett.* **60**, 937 (1988).
  - <sup>5</sup>H. Maeda, Y. Tanaka, M. Fukutumi, and T. Asano, *Jpn. J. Appl. Phys.* **27**, L209 (1988).
  - <sup>6</sup>R. J. Cava, B. Batlogg, J. J. Krajewski, R. Farrow, L. W. Rupp, A. E. White, K. Short, W. F. Peck, and T. Kometani, *Nature* **332**, 814 (1988).
  - <sup>7</sup>I. K. Schuller, D. G. Hinks, M. A. Beno, D. W. Capone II, L. Soderholm, J. P. Loquet, Y. Bruynseraede, C. U. Segre, and K. Zhang, *Solid State Commun.* **63**, 385 (1987).
  - <sup>8</sup>J. D. Jorgensen, M. A. Beno, D. G. Hinks, L. Soderholm, K. J. Volin, R. L. Hitterman, J. D. Grace, I. K. Schuller, C. U. Segre, K. Zhang, and M. S. Kleefisch, *Phys. Rev. B* **36**, 3608 (1987).
  - <sup>9</sup>H. M. O'Bryan and P. K. Gallagher, *Adv. Ceram. Mater.* **2**, 640 (1987).
  - <sup>10</sup>R. J. Cava, B. Batlogg, C. H. Chen, E. A. Rietman, S. M. Zahurak, and D. J. Werder, *Nature* **329**, 423 (1987).
  - <sup>11</sup>R. J. Cava, B. Batlogg, C. H. Chen, E. A. Rietman, S. M. Zahurak, and D. J. Werder, *Phys. Rev. B* **36**, 5719 (1987).
  - <sup>12</sup>R. Beyers, G. Lim, E. M. Engler, V. Y. Lee, M. L. Ramirez, R. J. Savoy, R. D. Jacowitz, T. M. Shaw, S. La Placa, R. Boehme, C. C. Tsuei, S. I. Park, M. W. Shafer, W. J. Gallagher, and G. V. Chandrashekhar, *Appl. Phys. Lett.* **51**, 614 (1987).
  - <sup>13</sup>D. de Fontaine, L. T. Wille, and S. C. Moss, *Phys. Rev. B* **36**, 5709 (1987).
  - <sup>14</sup>L. T. Wille and D. de Fontaine, *Phys. Rev. B* **37**, 2227 (1988).
  - <sup>15</sup>L. T. Wille, A. Berera, D. de Fontaine, and S. C. Moss, in *High-Temperature Superconductivity*, Proceedings of the Materials Research Symposia, edited by M. B. Brodsky, R. C. Dynes, K. Kitazawa, and H. L. Teller (Materials Research Society, Pittsburgh, 1988), Vol. 99, p. 535.
  - <sup>16</sup>A. Berera, L. T. Wille, and D. de Fontaine, *J. Stat. Phys.* **50**, 1245 (1988).
  - <sup>17</sup>L. T. Wille, A. Berera, and D. de Fontaine, *Phys. Rev. Lett.* **60**, 1065 (1988).
  - <sup>18</sup>A. Berera, L. T. Wille, and D. de Fontaine, *Physica C* **153-155**, 598 (1988).
  - <sup>19</sup>H. Bakker, D. O. Welch, and O. W. Lazareth, Jr., *Solid State Commun.* **64**, 237 (1987).
  - <sup>20</sup>E. Salomons, N. Koeman, R. Brouwer, D. G. de Groot, and R. Griessen, *Solid State Commun.* **63**, 1141 (1987).
  - <sup>21</sup>J. M. Bell, *Phys. Rev. B* **37**, 541 (1988).
  - <sup>22</sup>A. G. Khachatryan and J. W. Morris, Jr., *Phys. Rev. Lett.* **59**, 2776 (1987).
  - <sup>23</sup>A. G. Khachatryan, S. V. Semenovskaya, and J. W. Morris, Jr., *Phys. Rev. B* **37**, 2243 (1988).
  - <sup>24</sup>A. G. Khachatryan and J. W. Morris, Jr., *Phys. Rev. Lett.* **61**, 215 (1988).
  - <sup>25</sup>J. M. Sanchez, F. Mejia-Lira, and J. L. Moran-Lopez, *Phys. Rev. B* **37**, 3678 (1988).
  - <sup>26</sup>R. Kikuchi, *Phys. Rev.* **81**, 988 (1951).
  - <sup>27</sup>A. Berera and D. de Fontaine, *Phys. Rev. B* **39**, 6727 (1989).
  - <sup>28</sup>G. Van Tendeloo, H. W. Zandbergen, and S. Amelinckx, *Solid State Commun.* **63**, 603 (1987).
  - <sup>29</sup>H. W. Zandbergen, G. Van Tendeloo, T. Okabe, and S. Amelinckx, *Phys. Status Solidi A* **103**, 45 (1987).
  - <sup>30</sup>C. Chaillout, M. A. Alario-Franco, J. J. Capponi, J. Chénavas, J. L. Hodeau, and M. Marezio, *Phys. Rev. B* **36**, 7118 (1987).
  - <sup>31</sup>C. Chaillout, M. A. Alario-Franco, J. J. Capponi, J. Chénavas, P. Strobel, and M. Marezio, *Solid State Commun.* **65**, 283 (1988).
  - <sup>32</sup>M. Tanaka, M. Terauchi, K. Tsuda, and A. Ono, *Jpn. J. Appl. Phys.* **26**, L1237 (1987).
  - <sup>33</sup>D. J. Werder, C. H. Chen, R. J. Cava, and B. Batlogg, *Phys. Rev. B* **37**, 2317 (1988).
  - <sup>34</sup>R. M. Fleming, L. F. Schneemeyer, P. K. Gallagher, B. Batlogg, L. W. Rupp, and J. V. Waszczak, *Phys. Rev. B* **37**, 7920 (1988).
  - <sup>35</sup>C. H. Chen, D. J. Werder, L. F. Schneemeyer, P. K. Gallagher, and J. V. Waszczak, *Phys. Rev. B* **38**, 2888 (1988).
  - <sup>36</sup>D. J. Werder, C. H. Chen, R. J. Cava, and B. Batlogg, *Phys. Rev. B* **38**, 5130 (1988).
  - <sup>37</sup>A. T. Fiory, S. Martin, L. F. Schneemeyer, R. M. Fleming, A. E. White, and J. V. Waszczak, *Phys. Rev. B* **38**, 7129 (1988).
  - <sup>38</sup>D. de Fontaine in *Electronic Band Structure and Its Applications*, Vol. 283 of *Lecture Notes in Physics*, edited by M. Yusuf (Springer-Verlag, Berlin, 1987), p. 410.
  - <sup>39</sup>F. Ducastelle and F. Gautier, *J. Phys. F* **6**, 2039 (1976).
  - <sup>40</sup>A. Gonis, X. G. Zhang, A. J. Freeman, P. Turchi, G. M. Stocks, and D. M. Nicholson, *Phys. Rev. B* **36**, 4630 (1987).
  - <sup>41</sup>M. Sluiter and P. Turchi, in *Alloy Phase Stability*, Vol. 163 of *Nato Advanced Studies Institute, Series E: Applied Sciences*, edited by G. M. Stocks and A. Gonis (Plenum, New York, 1989).
  - <sup>42</sup>V. Heine and D. Weaire, *Solid State Phys.* **24**, 249 (1970).
  - <sup>43</sup>A. Berera, H. Dreyssé, L. T. Wille, and D. de Fontaine, *J. Phys. F* **18**, L49 (1988).
  - <sup>44</sup>H. Dreyssé, A. Berera, L. T. Wille, and D. de Fontaine, *Phys. Rev. B* **39**, 2442 (1989).
  - <sup>45</sup>M. A. Alario-Franco, C. Chaillout, J. J. Capponi, and J. Chénavas, *Mater. Res. Bull.* **22**, 1685 (1987).
  - <sup>46</sup>M. A. Alario-Franco, C. Chaillout, J. J. Capponi, J. Chénavas, and M. Marezio, *Physica C* **156**, 455 (1988).
  - <sup>47</sup>B. M. McCoy and T. T. Wu, *The Two-dimensional Ising Model*, (Harvard University Press, Cambridge, 1973).
  - <sup>48</sup>J. A. Barker, *Proc. R. Soc. London, Ser. A* **216**, 45 (1953).
  - <sup>49</sup>J. Hijmans and J. de Boer, *Physica* **21**, 471 (1955).
  - <sup>50</sup>J. M. Sanchez and D. de Fontaine, *Phys. Rev. B* **21**, 216 (1980).
  - <sup>51</sup>J. M. Sanchez, F. Ducastelle, and D. Gratias, *Physica* **128A**, 334 (1984).
  - <sup>52</sup>D. de Fontaine, in *Alloy Phase Stability*, Vol. 163 of *Nato Advanced Studies Institute, Series E: Applied Sciences*, edited by G. M. Stocks and A. Gonis (Plenum, New York, 1989).
  - <sup>53</sup>S. M. Allen and J. W. Cahn, in *Alloy Phase Diagrams*, Proceedings of the Materials Research Symposia, edited by L. M. Bennett, T. B. Massalski and B. C. Giessen (Materials Research Society, Pittsburgh, 1983), Vol. 19, p. 195.
  - <sup>54</sup>E. D. Specht, C. J. Sparks, A. G. Dhere, J. Brynstad, O. B. Cavin, D. M. Kroeger, and H. A. Oye, *Phys. Rev. B* **37**, 7426 (1988).
  - <sup>55</sup>J. Zaanen, A. T. Paxton, O. Jepsen, and O. K. Andersen, *Phys. Rev. Lett.* **60**, 2685 (1988).
  - <sup>56</sup>N. C. Yeh, K. N. Tu, S. I. Park, and C. C. Tsuei, *Phys. Rev. B* **38**, 7087 (1988).
  - <sup>57</sup>K. F. McCarty, J. C. Hamilton, R. N. Shelton, and D. S. Ginley, *Phys. Rev. B* **38**, 2914 (1988).
  - <sup>58</sup>H. You, J. D. Axe, X. B. Kan, S. Hashimoto, S. C. Moss, J. Z. Liu, G. W. Crabtree, and D. J. Lam, *Phys. Rev. B* **38**, 9213 (1988).
  - <sup>59</sup>Y. Tokura, J. B. Torrance, T. C. Huang, and A. I. Nazzari, *Phys. Rev. B* **38**, 7156 (1988).